THE ASTROPHYSICAL JOURNAL, **199**:265–281, 1975 July 1

THE STRUCTURE AND EVOLUTION OF JUPITER: THE FLUID CONTRACTION STAGE*

HAROLD C. GRABOSKE, JR.,† JAMES B. POLLACK,‡ ALLAN S. GROSSMAN,§ AND ROBERT J. OLNESS†
Received 1973 July 13; revised 1974 December 9

ABSTRACT

An evolutionary study of a 0.00095 $M_\odot$ star, composed of a convective, adiabatic, homogeneous fluid, has been performed using stellar structure methods. A new numerical technique is used to calculate model atmospheres in the form of time-average vertical temperature structures, including all relevant opacity sources and a solar energy deposition component. Thermodynamic properties for pure hydrogen and a solar mixture ($X = 0.74$, $Y = 0.24$, $Z = 0.02$) are developed for $-7 \leq \log \rho$ (g cm^{-3}) ≤ 1 and $1.78 \leq \log T$(K) ≤ 4.78, utilizing recent high-pressure experimental results and new theoretical methods. The resultant gravitationally contracting evolutionary models exhibit two phases. An early stellar phase, behaving like a typical low-mass pre–main-sequence object, has high luminosities which have left a record in the structure of the Galilean satellites. This phase also has high internal temperatures, $(T_c)_{\max}$ reaching 51,400, which ensures a long subsequent evolution as a fully mixed, convective structure. The second phase is an approach to a degenerate dwarf cooling curve, which gives excellent agreement with the observed radius and luminosity of Jupiter. A short time scale for the standard adiabatic fluid models (2.6×10^9 years) is extended by combinations of several factors influencing the planetary evolution. An analysis of the sensitivity of evolution to chemical composition, solar energy deposition, equation of state, model atmospheres, and superadiabaticity demonstrates that equation of state and superadiabaticity have the strongest influence over planetary time scales.

Subject headings: interiors, planetary — Jupiter

I. INTRODUCTION

Efforts to understand the structure and evolution of the giant planets may be expected to increase substantially under the influence of *Pioneer* space probe observations of Jupiter. Interest in these outer planets was strongly stimulated in 1969 by Aumann, Gillespie, and Low's remarkable observation that Jupiter radiates 2.7 times more energy than it receives from the Sun. Prior studies have been primarily concerned with two questions about the giant planets. First, what is their present structure? A complete answer to this question involves knowledge of the internal temperature distribution, the chemical composition (or hydrogen-to-helium ratio), the source of the excess flux, the source of the intense Jovian magnetic field, and the state of chemical fractionation in the interior. The second question concerns events 4.5 billion years ago, and asks, how did the giant planets form? In this study, we shall attempt to show that a quantitative answer to the first question must involve a complete evolutionary analysis of Jupiter, from early in its existence to the present day. The answer to the second question is not sought, but its importance and relation to the study of the present planet is indicated.

The seminal study of giant planet structure is that of DeMarcus (1958) who established a complete set of thermodynamic properties of cold hydrogen and helium, and then applied this theory to the construction of static models of Jupiter and Saturn. The results established the nearly solar composition of both planets and gave good agreement with the observational variables. A subsequent investigation by Peebles (1964) used solutions of the static structure equations together with warm adiabatic convective envelopes. The results of these two studies produced the accepted model of giant planet structure: a dense small core (metals or pure helium) surrounded by an extensive warm core of homogeneous solid hydrogen-helium, and an outer deep adiabatic envelope. The overall composition approximates the solar mixture.

The discovery of the excess heat flux led Hubbard (1968, 1969) to propose a quite different structure for Jupiter. His proposed models are warm, fully mixed, adiabatic convecting fluids. The excess energy flux is due solely to gravitational contraction, the energy radiated from either a current epoch contraction or from stored internal energy derived from a prior contraction. This model for the present Jupiter has been studied in some detail (Hubbard 1969, 1970) and represents the most complete treatment of the planet to date. Several other mechanisms proposed to explain

* Work performed under the auspices of the U.S. Atomic Energy Commission.

† Lawrence Livermore Laboratory, University of California.

‡ NASA-Ames Research Center, Moffet Field, CA.

§ Iowa State University, Ames.

the excess flux have been ruled out, as they are quantitatively inadequate by orders of magnitude. These include accretion of interplanetary debris (Newburn and Gulkis 1971), natural radioactivity (Hubbard and Smoluchowski 1973), gradual change of the gravitational constant (Smoluchowski 1972), low-temperature nuclear fusion (Grossman *et al.* 1972), and secular albedo change (Hubbard and Smoluchowski 1973). An evolutionary generalization of Hubbard's static model of a convective fluid undergoing gravitational contraction is the subject discussed in this paper. We propose that such a system (with modifications, to be dealt with in detail) represents the central stage of giant planet evolution, a stage that ensues early in the existence of the planet and lasts for a substantial fraction of its total lifetime. In this proposed evolutionary sequence, the fluid contraction stage has both prior and subsequent stages; some very difficult questions must be answered to understand these early and late phases.

The early evolution problem concerns the "assembly" stage of planetary formation. The most obvious source of a fluid stellar configuration such as Hubbard proposes is a protostar, a gravitationally collapsing condensation in the outer solar nebula. This "hot" origin is reasonably well understood, and, in principle, a complete calculation could be carried out to describe the dynamic and quasi-static stabilization processes. However, a serious objection to this protostar origin for Jupiter has been made by Hills (1971), who cites the difficulty of forming a stable condensation in the primordial solar nebula in the presence of strong solar tidal forces. If this objection is valid, then a "cold" origin for the giant planets is indicated. Models for a cold origin have been proposed in the form of accretion of a cold solid (Hills 1971) and condensation of a cold liquid (Horedt 1972). The resolution of this problem is not attempted here; the quantitative determination of the giant planet assembly or formation will be quite difficult. In spite of this present uncertainty, we propose (§ IV) that either origin—protostar or cold—will result at some early solar system epoch in a hot, fully mixed, fluid convective stellar configuration, with a radius substantially larger than that of Jupiter. Further, several observational features of the Jovian system will be cited to support this contention.

The formation or assembly stage is succeeded by the fluid convective stage, an evolutionary sequence of initially stellar form which gravitationally contracts into the planetary configuration of present day Jupiter. All prior studies of Jupiter have used static models, nonevolving configurations constructed by fitting methods. These methods use the observed mass, radius, and surface temperature to fit model atmospheres to molecular-metallic interiors. The standard approach in studying an evolving star is to specify only the total mass and chemical composition; these two parameters then allow the determination of the entire evolutionary history of the star, predicting internal structure and external (observable) characteristics at all times. In a previous paper (Grossman *et al.* 1972) the evolution of a 0.001 $M_\odot$ star composed of pure hydrogen was calculated to determine the feasibility of a stellar structure approach and to define the relevant details of an evolving very low mass object. The stellar configuration contracted gravitationally from 35 Jovian radii (R_J) for 10^9 years, at which time it had a radius of 2.8 R_J and a luminosity 2.5 times Jupiter's measured emission. Its behavior closely resembled the early evolution of low-mass stars in the range 0.01–0.05 $M_\odot$ (Grossman and Graboske 1973), exhibiting an initially increasing internal temperature which reaches a maximum central temperature dependent on total mass, followed by rapid cooling onto a degenerate "black" dwarf cooling curve.

Our object in this paper is to determine, using improved model atmosphere calculations and substantially improved thermodynamic properties for hydrogen and hydrogen-helium fluids, the complete evolution of a fluid contracting star of Jovian mass. This effort attempts to answer two key questions. First, can this type of model produce an object which agrees with all the large-scale observational characteristics of Jupiter? Second, if not, what modifications are required to produce such a model? It is at this point that the second problem area becomes relevant—i.e., the nature of the current stage of Jovian evolution. If the gravitational energy, both current and stored, of the fluid contraction stage is insufficient to explain the present Jovian flux, an additional energy source is required. Two sources have been proposed, which by their nature would naturally succeed the fluid contraction stage. Smoluchowski (1970) has proposed that the present Jupiter contains a zone of solid hydrogen, having frozen from the fluid mixture as the planet cooled, and that neutral helium fluid is diffusing inward from the metallic hydrogen lattice under the influence of the gravitational field. Salpeter (1973) proposes a similar gravitational fractionation, the neutral helium fluid becoming immiscible with the metallic hydrogen fluid and diffusing toward the center, releasing a substantial amount of additional gravitational energy. Although the theoretical details required to substantiate these proposed mechanisms are not developed yet, they do represent feasible processes whose initiation would terminate the fluid contraction stage. These mechanisms can be temporarily defined as a post–fluid contraction stage of late evolution, whose actual existence depends on the demonstration that the fluid contraction stage is inadequate to describe the present state of Jupiter. They further depend on a careful determination of the structure and evolution of this prior stage to allow accurate estimates of energy and lifetime requirements.

The observational properties of Jupiter used as standards of comparison for the theoretical results are taken from Newburn and Gulkis (1973):

$$\left.\begin{array}{ll}\text{Mass:} & M_J = 0.00095\, M_\odot \\ \text{Radius:} & R_J = 7.014 \times 10^9\ \text{cm}\end{array}\right\} \begin{array}{l}\langle \rho_J \rangle = \\ 1.314\ \text{g cm}^{-3},\end{array}$$

Effective temperature: $(T_e)_J = 134 \pm 4$ K,

Luminosity: $L_J = 1.805 \times 10^{-9} L_\odot$ (for $T_\odot = 105$ K),

Age: $t_J = 4.5 \times 10^9$ years.

The basic assumptions of the evolution calculation are: (1) The interior is homogeneous at all times. (2) Energy transport is convective throughout the interior. (3) Effects of rotation and magnetic fields are neglected. (4) The models are spherically symmetric.

The validity of these assumptions will be examined in the final section of the paper. In § II, the construction of the model atmospheres is described, followed by a summary of the thermodynamic properties and a brief description of the evolutionary stellar structure method. The results of the evolutionary calculations are presented in § III, and a discussion and conclusions are given in § IV.

II. CONSTITUTIVE PHYSICS

a) *Model Atmospheres*

A series of model atmospheres was calculated to determine one of the outer boundary conditions to which the interior solutions are matched. Below we describe the sources of opacity for our model atmospheres, the manner in which they were calculated, and the way they were used in the main calculation.

Because the effective temperatures of interest are less than 2000 K, all the gases in the atmosphere for a system composed of a solar composition are in the form of molecules, and the principal sources of opacity are hydrogen, ammonia, water vapor, and methane. Hydrogen is the chief source of opacity for effective temperatures below 150 K; hydrogen and ammonia for values between 150 K and 300 K; and water vapor at higher temperatures. We divided the thermal infrared into 30 spectral regions and within each region used the transmission average opacity formulae given by Pollack (1969) to describe the opacity properties of each species.

The hydrogen opacity, which arises from translational, rotational, and vibrational pressure-induced transitions, was derived from Trafton's (1967) formulae and Linsky's (1969) calculations. The hydrogen absorption is proportional to the square of the pressure. The remaining opacity sources involve permitted transitions. For this type of opacity to be important within a given spectral region implies that the centers of the individual rotational lines are saturated and that the absorption lies within the strong line region, where the transmission average opacity varies as the square root of gas amount and pressure. The absorption coefficients of water vapor were obtained from Ferriso, Ludwig, and Thomson (1966); those of methane from Burch *et al.* (1962); and those of ammonia from Gille and Lee (1969) and France and Williams (1969). In the case of hydrogen and water vapor at all wavelengths and of ammonia longward of 7 μ, allowance was made for the temperature dependence of the absorption coefficients.

In regions where they were not frozen out, we used solar abundance values for the amounts of oxygen, carbon, and nitrogen relative to hydrogen and assumed that these elements were entirely in the form of water vapor, methane, and ammonia, respectively. At temperatures below the freezing point of a given species, the gas was assumed to follow its saturation vapor pressure curve and its latent heat was factored into the calculation of the adiabatic lapse rate.

To determine the temperature structure of the upper atmosphere, i.e., the region which radiates to space, we used a local radiative-convective model. A numerical procedure was used to determine the temperature profile, which was consistent with a specified net flux at those levels in the atmosphere which were in radiative equilibrium. At levels where the computed radiative temperature gradient exceeded the adiabatic values, the adiabatic value was used and these regions were in convective equilibrium.

The numerical method used to compute the model atmospheres is described in detail by Pollack and Ohring (1973) and Grossman *et al.* (1972). Briefly, this procedure consists of making an initial guess as to the temperature structure and using a flux corrective method to determine the actual temperature structure. Each iterative cycle consists of calculating the net radiative fluxes implied by the present temperature structure and then obtaining an improved set of temperature values from the difference between the computed and desired fluxes. This cycle is repeated until the flux residuals are less than a few percent. The final computed temperature structure is accurate to better than a percent, if we exclude the errors attached to the input data, such as the opacity coefficients. All the computed atmospheres are characterized by a radiative zone at lower pressure levels and a convective zone beneath.

In addition to the flux supplied at the top of the atmosphere from the interior, there is also a component of the flux due to absorption of sunlight. An interesting consequence of the presence of this solar flux component is that the surface temperature can never be less than the effective temperature due to the solar component. Thus, the later stages of evolution of a Jovian type planet may be quite different from that of an isolated, low-mass star. No explicit calculation of the solar energy deposition profile was made. We assumed that it was all deposited below the levels dealt with. The solar energy deposited in the surface layers and subsequently reradiated to space will be characterized by an effective blackbody temperature $T_{\odot}$. The effective temperature due to the solar component has a range of uncertainty in value due to the current uncertainty in our knowledge of the bolometric albedo of Jupiter. In deriving $T_{\odot}$, we assumed that the bolometric albedo has limiting values of 0.3 and 0.65. This range was based on the observed geometric albedos of Jupiter (Irvine *et al.* 1968) and estimated values of the as yet unobserved phase integral of between 0.75 and 1.75. The time-average value of the solar constant, also required in the determination of insolation temperature, was set equal to 85 percent of its present value (Ezer and Cameron 1963). The resulting minimum, most probable, and maximum values of $T_{\odot}$ corresponding to high, average, and low albedo limits are 89, 102, and 108 K.

The result of each model atmosphere calculation is a determination of the temperature value at a specified pressure level within the convection zone. The interior solutions are matched to these temperature-pressure pairs. The calculations were carried out over a two-dimensional grid involving the value of the surface gravity (and hence the radius) and effective temperature. Because at a fixed value of effective temperature the models change in a very simple manner with changing surface gravity, it was sufficient to perform the computation for only two values of surface gravity. To a very good approximation the temperature structure remains the same when the pressure levels are scaled as the square root of the gravity. Table 1 summarizes the values of the temperature-pressure points as a function of effective temperature and gravity for models having solar proportions of hydrogen and helium. A similar set of model atmospheres was derived for the calculations of a pure hydrogen composition. The actual fitting point for a given contraction model calculation was found by interpolating within the grid of model atmosphere values.

An additional set of model atmospheres was calculated based on a modification of the solar mix results. To test the sensitivity of our evolutionary calculations to possible errors and changes in the atmospheres, a modified model atmospheres (MATM) set was developed. Since the chemical equlibria and related molecular opacities for the radiative zone are believed to be fairly well known, the possible future modifications are small. Based on an analysis of the errors and uncertainties in the relevant variables and in the numerical procedures, the MATM atmospheres had pressures increased by a factor which increased from a minimum of 10 percent to a maximum of 20 percent as a function of temperature over the standard results of Table 1. This modified set of MATM values was then used in the model calculations in place of the standard values.

b) *Thermodynamic Properties*

The thermodynamic properties requires for the stellar structure calculation include the pressure and enthalpy equations of state, with their derivatives, combined to yield second-order thermal properties such as ∇_{ad}, C_p, and $(\partial \ln \rho/\partial \ln T)_p$. The range of density and temperature for which these quantities are needed must include all regions encountered by the evolving planetary model. From prior evolutionary studies of low-mass stars together with Hubbard's static models of Jupiter, a range of $10^{-7} \leq \rho(\mathrm{g\ cm^{-3}}) \leq 10^1$ and $60 \leq T(\mathrm{K}) \leq 60{,}000$ was chosen. Two chemical compositions were chosen: pure hydrogen (H) consisting of six possible species (H_2, H_2^+, H^-, H, H^+, e^-) and a solar mixture (S1) composed of H, He, C, N, O, Ne with 20 species participating in the equilibrium. The S1 solar mixture ($X = 0.74$, $Y = 0.24$, $Z = 0.02$) uses Allen's (1963) solar metal composition.

The detailed discussion of the thermodynamic theory is given by Graboske, Olness, and Grossman (1975), and the result is two sets of tables including pressure, enthalpy, ∇_{ad}, and the other required properties for a skewed (ρ, T)-grid having the limits determined above. In addition to the H and S1 thermodynamic properties, to further examine the quality of the physical models presented here, the thermodynamic properties of the S1 solar mixture were perturbed away from the "best" values of the final model. This modified thermodynamic properties set (MTDP) with its known differences is then used in the evolutionary calculations, and the sensitivity of the

TABLE 1

MODEL ATMOSPHERES

	Gravity = 40.39 cm s^{-2} (8 R_J†)		Gravity = 2585 cm s^{-2} (1 R_J)	
Effective Temperature	Pressure (atm)	Temperature (K)	Pressure (atm)	Temperature (K)
20.00......	0.2238	25.22	1.79	25.02
60.00......	0.16	76.17	1.28	76.24
100.00......	0.16	142.9	1.28	141.3
150.00......	0.16	235.9	1.28	232.2
200.00......	0.16	338.4	1.28	332.3
250.00......	0.16	410.1	1.28	406.9
300.00......	0.16	486.8	1.28	486.4
400.00......	0.16	643.3	1.28	643.3
500.00......	0.16	807.6	1.28	807.6
600.00......	0.16	957.9	1.28	957.9
700.00......	0.16	1093.0	1.28	1093.0
900.00......	0.16	1412.0	1.28	1412.0
1100.00......	0.16	1754.0	1.28	1754.0
1300.00......	0.16	2111.0	1.28	2111.0
1500.00......	0.16	2528.0	1.28	2528.0
1700.00......	0.16	2999.0	1.28	2996.0
1900.00......	0.16	3532.0	1.28	3540.0

* Contains both solar and interior contributions.

† Gravity value when Jupiter was 8 times its present size.

model structure to known changes in the physics can be examined.

From the analysis of Graboske *et al.* (1975), as well as fundamental theoretical considerations, it is possible to define a region of probable error for the physics. Specifically, the low-density model has been validated to densities approaching 0.1 g cm^{-3} and asymptotically approaches the ideal gas at low density and the ideal plasma at high temperature. The high-density model asymptotically approaches the ideal Fermi gas at high density and is in good agreement with the Monte Carlo model at densities approaching 1 g cm^{-3}. Obviously, there is no sense in perturbing an equation of state where it is known to be valid. Therefore the modification region was centered on the intermediate zone, which ranges from 0.1 to 1 g cm^{-3} for 10^3 K $\leq T \leqslant$ 20,000 K.

The thermodynamic properties were modified in a manner which changes them in the direction of better agreement with Monte Carlo metallic fluid results. This was done by multiplying the pressures and energies in the intermediate zone by a bivariate Gaussian in ρ and T:

$$P = P(1 + F_P)\,, \qquad E = E(1 + F_E)\,,$$

$$F_i = K_i \exp\left[-(\log \rho/\rho_0/\log \rho_w)^2\right] \exp\{-[T - T_0/T_w]^2\}\,,$$

where $\rho_0 = 0.3162$ g cm^{-3}, $\rho_w = 5$, $T_0 = 4000$ K, $T_w = 16{,}780$ K. This gave a modified region ranging in density from the unperturbed values at 0.01 and 10 g cm^{-3} to a maximum change at 0.3162 g cm^{-3}. The modified temperature range starts at the minimum T in the table (1000 K at 1 g cm^{-3}), maximizing at 4000 K and decreasing to the unperturbed values at 40,000 K, where both high- and low-density theories are in good agreement. The size and magnitude of the perturbations, K_P and K_E, were set equal to -0.5 and $+0.25$, respectively, values chosen from the estimated errors found in the analysis of Graboske *et al.* (1975) and from considerations of the distortions required to give closer agreement between Hubbard's pure Monte Carlo theory (Hubbard and Slattery 1971; Hubbard 1972) and the interpolated values. Thus, the maximum perturbations of the S1 pressures and energies (multiplicative factors of 0.5 and 1.25, respectively) occur at 0.3162 g cm^{-3} and 4000 K. These modified equations of state were then used to develop the additional thermodynamic properties required, such as enthalpy and ∇_{ad}, and this thermodynamic set was used to construct the MTDP sequence of models, as discussed in § III.

c) *Stellar Structure Calculations*

The interiors of the stellar models are calculated by the Henyey method as described by Kippenhahn, Weigert, and Hofmeister (1967) with the point $M_r = 0.97\, M_{\text{TOT}}$ chosen as the point where the surface boundary condition is applied (hereinafter referred to as the core boundary or fitting point). The surface boundary condition for the interior solution consists of the values of ρ, T, R, and L_r at the fitting point as determined by an inward integration from the surface of the model. The surface boundary condition is fitted to interior models by the triangular method given by Kippenhahn *et al.*

The surface boundary layer solution consists of two major zones. The outer zone solution, described in § II, provides the (temperature, pressure)-distribution down to approximately $T = T_e$ assuming constant g and net flux (σT_e^4). This zone contains an outer radiative equilibrium part and an inner convective part. The inner zone of the surface boundary layer is a convective zone, starting with a (P, T)-point from the upper zone and the values for the total mass, radius, and luminosity. The stellar structure equations,

$$d \log T/d \log P = \nabla\,,$$

$$d \log r/d \log P = -rP/GM_r\rho\,,$$

$$d \log M_r/d \log P = -4\pi r^4 P/GM_r^2\,,$$

are then integrated inward at constant luminosity by the Runge-Kutta method to the fitting point. The choice of ∇ for this convection zone is crucial to the structure and evolution of the configuration. The simpler choice, made in all studies of the giant planets, is that the transition from the radiative zone to a highly effective convective zone is very rapid. If this is assumed, then the energy transport is by adiabatic convection, and the appropriate temperature gradient is the adiabatic gradient, $\nabla = \nabla_{\text{ad}}$. This choice is used for the major portion of our study; however, the alternative assumption of inefficient convection—that is, a superadiabatic convection zone—is investigated in an approximate way.

Since the temperature gradient throughout most of the mass of these fully convective objects will be close to the adiabatic gradient, the luminosity and effective temperature will be essentially determined by the thin surface layer. The outer part of the surface boundary layer above $T = T_e$ will be in radiative equilibrium. Within this radiative layer it will be both the opacity and insolation energy which are dominant factors controlling the amount of energy that can be radiated by the star. For a given radius, the higher the opacity and/or the lower the insolation, the smaller the amount of energy radiated, and thus the lower the luminosity and the slower the contraction or cooling rate.

III. RESULTS OF THE EVOLUTIONARY CALCULATIONS

a) *Structure and Evolution of the Standard Model*

Combining the constitutive physics with the star code, a series of evolutionary model sequences were calculated for a star of mass 0.00095 $M_\odot$. The standard model, which will serve as a reference sequence for

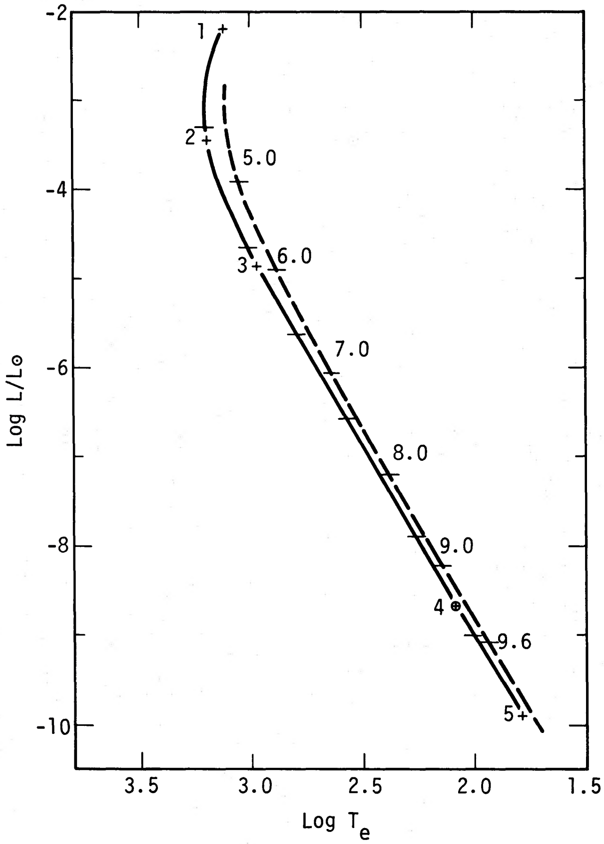

FIG. 1.—The theoretical (log L, log T_e)-track for the S1 standard sequence (———) with $T_\odot = 102$ K. The value of log t in years is indicated by the horizontal bars, while model epochs 1–5 are shown (+), as is the observational value for Jupiter ⊕. The corresponding hydrogen sequence is given by the broken line (– – –).

comparison with observations and other theoretical models, is composed of a mixture based on the solar composition. The star is assumed to be fluid throughout, completely convective except for a thin radiative zone in the atmosphere, completely adiabatic, and fully mixed, and the solar energy deposition is given by $T_\odot = 102$ K.

The resulting evolutionary sequence is started from an initial position at 16 R_J and is evolved until a lifetime of approximately 10^{10} years is reached. The evolution can be characterized as two separate phases, the first being that of a typical low-mass star evolving along the Hayashi track followed by a rapid transition to the cooling curve of a degenerate cold object. These phases will be discussed separately and for simplicity will be referred to as the stellar phase and the degenerate phase. At the beginning of the stellar phase, the models are large-radius R, high-luminosity L, high-T_e objects. They evolve down the Hayashi track rapidly at first, with almost constant T_e and strongly decreasing L and R. The stellar phase is identical to that observed for low-mass stars ($M/M_\odot \leq 0.20$); during this phase the interior is hot

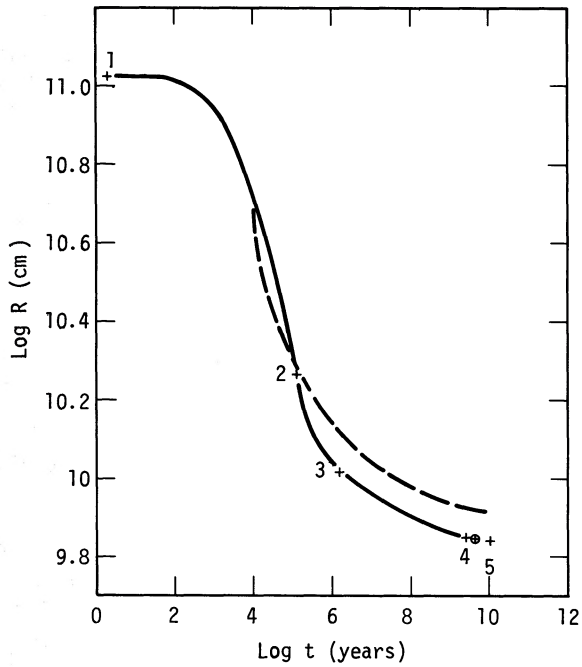

FIG. 2.—Time dependence of radius for the S1 standard sequence, with epochs 1–5 (+) and Jupiter (⊕) indicated. The broken line (– – –) gives the radius of the hydrogen sequence.

(15,000–50,000 K), with hydrogen, and at one point helium, substantially ionized through the interior.

The behavior of the observable model variables, R, L, and T_e are shown in Figures 1, 2, and 3. A notable feature of the stellar phase is the substantial period of high luminosity and effective temperature. As shown in Figure 1, for times of 10^6 years, the model has $1050 \leq T_e(\mathrm{K}) \leq 1600$ and $-4.6 \leq \log L/L_\odot \leq$

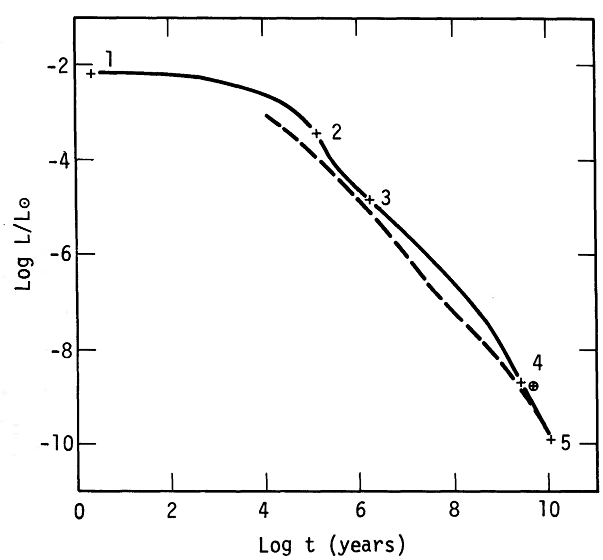

FIG. 3.—Time dependence of luminosity for the S1 standard sequence, with epochs 1 to 5, the Jovian luminosity and the hydrogen sequence shown as in Fig. 2.

-2.2. The mean luminosity from 0.1×10^6 to 1×10^6 years is $10^{-4}\, L_\odot$, and the value of log L at the top of the track is equal to that of a $0.15\, M_\odot$ main sequence M dwarf. This high-luminosity phase exists even if model evolution is started at a much smaller initial radius. With an initial model of only $3.5\, R_J$ the initial luminosity would be log $L/L_\odot = -3.1$ and log T_e = 1600 K. In these figures, there are five specific epochs defined which span the entire evolutionary sequence and represent special features. Epochs 1 and 2 are stellar phase models, corresponding respectively to the initial model at the top of the Hayashi track and to the central temperature maximum. Epoch 3 is a transition model at log t(years) = 6.21 where the stellar phase has been succeeded by the degenerate phase. Epochs 4 and 5 are advanced degenerate phase models, epoch 4 at 2.6×10^9 years corresponding most closely to the observational values for Jupiter, and epoch 5 at 1×10^{10} years being the end of the standard S1 sequence. In Figures 2 and 3, the time variation of R and L are illustrated. The transition from stellar phase to degenerate phase produces evident changes in the time dependence of both variables, occurring just subsequent to epoch 2.

The internal structure of the standard S1 model is illustrated in Figures 4 and 5. The most notable feature of the stellar phase interiors is the high temperatures reached. As shown in Figure 4, the central temperature of the model increases steadily from an initial value of 15,600 K until at log t = 5.08 a maximum value of 51,400 K is reached. An abrupt and accelerating decrease following this maximum produces a temperature-time history identical to that found in low-mass stars in the range $0.01 \leq M/M_\odot \leq 0.20$. This high temperatures extends throughout the entire

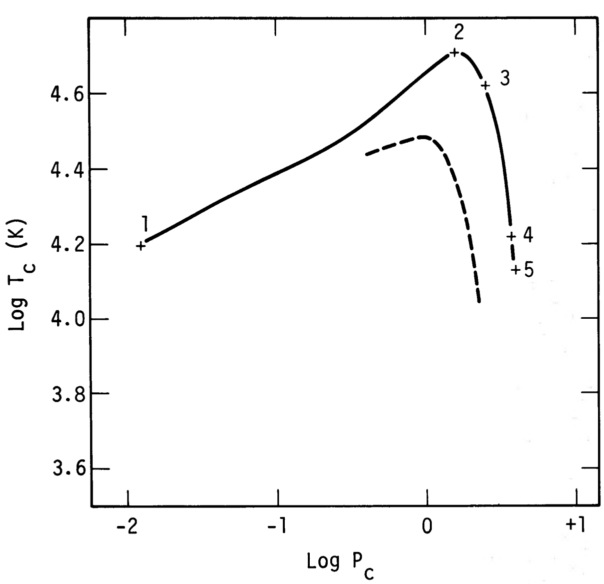

FIG. 4.—Variation of central temperature and density for the S1 standard sequence, with epochs 1–5 and the hydrogen sequence shown as in Fig. 2. The time to $T_{\max}$ is 1.22×10^5 years for the S1 sequence, and 7.76×10^5 years for the H sequence.

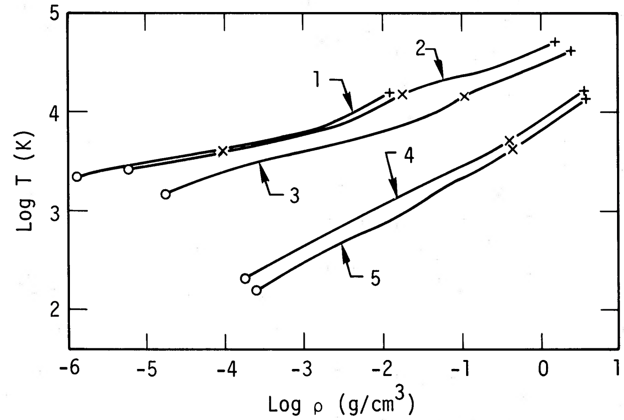

FIG. 5.—Structure lines for the S1 standard sequence ($T_\odot$ = 102 K) at five evolutionary stages. The run of density and temperature is shown for each epoch, with the center (+), core boundary (×) and surface (⊙) indicated.

interior, the mean temperature at epoch 2 being about 37,500 K, and the high internal temperature phase is very long, T_c not falling below 20,000 K for 10^9 years. Note also that starting the model evolution at a much smaller radius (for example, $R = 3.5\, R_J$) results in a T_c = 50,100, only 300 K cooler than $T_{\max}$. This spatially extensive and long high-temperature phase could produce a fully mixed, homogeneous object regardless of the inhomogeneities or fractionation occurring in the assembly of the protostar. The strong thermal gradients and resultant strong convective flow will vaporize and fully mix any primordial solid components. A more detailed picture of the structure of the model sequence is exhibited by the structure lines for the five epochs shown in Figure 5. The stellar phase models (epochs 1 and 2) show a typical completely convective structure, with a diffuse extended envelope and a hot expanded core. The temperature gradient in the central regions at epoch 1 is noticeably steeper than at epochs 2 and 3; it is in this early period where maximum temperatures may be expected to induce strong convective flow over the entire interior that complete interior mixing will probably occur. The central and core boundary ($M_r/M = 0$ and $M_r/M = 0.97$, respectively) densities increase markedly between epochs 1 and 2, while the outer layers are only slightly affected. Epoch 3 is a transition to the beginning of the degenerate phase and has a different structure: the interior (center to core boundary) has condensed considerably, having only half the density range of the epoch 2 model. The temperature gradient has also steepened, presaging the metallic fluid temperature gradients in the interiors of the degenerate phase models. The surface layers at epoch 3 have begun their cooling and are an order of magnitude denser than at epoch 2.

The second evolutionary phase, the contracting degenerate fluid, covers the time period $6.20 \leq \log t \leq 10$, which is 0.9975 of the total lifetime. Both the internal structure and the external observable variables behave very differently in this phase. Starting from the epoch 3 values $\log L/L_\odot = -4.84$, $\log R = 10.017$, and $\log T_e = 2.964$, the model sequence cools and contracts along a line asymptotically approaching the zero-temperature cooling curve for S1 composition and a 0.00095 $M_\odot$ mass. In Figure 1, the slope of the track in the ($\log L$, $\log T_e$)-plane is -4.15 in the 1×10^9 to 1×10^{10} year period. As seen in Figure 2, the radius drops steeply near epoch 3, and by epoch 4 the rate of contraction is much slower. For example, at epoch 4 the rate of contraction is $dR/dt = 0.761$ mm year^{-1}; this rate occurs near the epoch where the model radius and luminosity closely approach the observed Jovian values.

The luminosity decreases with time, as shown in Figure 3, where $\log L/L_\odot$ is roughly linear in $\log t$ over the period $5 \leq \log t \leq 8.5$, with an approximate slope of -1.3. The most interesting feature of the theoretical H-R diagram (Fig. 1) is that the evolutionary track passes almost exactly through the point representing $(T_e)_J$ and L_J. This striking agreement is achieved by specifying only the mass and chemical composition. The best match of the theoretical model to Jupiter's observed values is at $\log T_e = 2.083$ (this is $T_e = 121$ K, which when combined with a solar contribution of $T_\odot = 102$ K yields an observed T_e of 134 K) and $\log L/L_\odot = -8.705$, higher by 2 percent than the observed luminosity.

In addition to these quantities, three other observational variables should be compared. The first two gravitational moments are presently considered the most sensitive tests of model accuracy for Jupiter. Since the spherical model used here cannot be tested in this way, these moments are not useful here. A subsequent study will contain an analysis of a rotating, oblate model utilizing the structure and constitutive physics of this study. It is perhaps relevant that the structure and physics used here are qualitatively similar to those used by Hubbard (1970). In both cases there is a fully fluid object, with an 80 percent (by radius) metallic-hydrogen fluid core, so it is not unlikely that the moments for rotating nonspherical models based on our physics will be reasonably close to Hubbard's values, which are in good agreement with the observations.

A major difficulty in determining whether the standard S1 model sequence of fluid convective contracting models actually represents the true model of the planet Jupiter lies in the ages or lifetimes of the models. The theoretical model which gives best agreement with R_J and L_J has an age of 2.6×10^9 years, far less than the accepted value of 4.5×10^9. There are numerous explanations to account for such a difference, but we shall defer these to § IV and remark here that the sensitivity analysis of § III*b* will provide more information about the time scale problem. The standard S1 model then gives excellent agreement with Jupiter at a 2.6×10^9 year epoch. At 4.5×10^9 years, the sequence has a radius exactly equal to R_J and a luminosity 2.4 times smaller than L_J.

The internal structure of the degenerate phase models corresponding to the above evolutionary period is illustrated in Figures 4 and 5. The track of the model centers (Fig. 4) shows a continuing and substantial cooling, T_c decreasing from 41,800 K at epoch 3 to 16,500 K at epoch 4 and 13,500 K at the end of the track. The central density during the degenerate phase increases from 2.4 g cm^{-3} (epoch 3) to 3.7 g cm^{-3} (epoch 4) and 3.8 g cm^{-3} at 10^{10} years. The behavior of the entire interior in this phase can be described as steady slow cooling (3000 K in 7.5 $\times 10^9$ years from epoch 4 to epoch 5) at nearly constant density. The small density increase is a direct reflection of the very slow rate of contraction mentioned above. The detailed model structure during the degenerate phase is seen in Figure 5. By epoch 4 the model has reached its limiting fluid contraction structure; all interior points follow the behavior of the center, even the core boundary. The envelope exhibits little structure, with the surface density and temperature varying only slightly over the 2 to 8 $\times 10^9$ year period. The values for a 2.6×10^9 year model, $T_c = 16{,}500$ K, $\rho_c = 3.7$ g cm^{-3}, are somewhat hotter than early models obtained by Hubbard (1970), $T_c = 7300$ K, $\rho_c = 4.23$ g cm^{-3}, for a static-fluid adiabatic nonspherical model having a different composition ($X = 0.66$) and different interior physics.

The distribution of the thermodynamic variables as a function of mass for a degenerate phase model (epoch 4) is given in Figure 6. The behavior shown here is representative of the entire degenerate phase, specifically from 10^8 to 10^{10} years. The main point is the relatively small decrease in the temperature from center to core boundary; the temperature at $M_r/M = 0.97$ is 0.3 times T_c. The density and pressure fall off relatively slowly also.

An additional feature distinguishing the stellar and degenerate phases of the evolutionary sequence is the

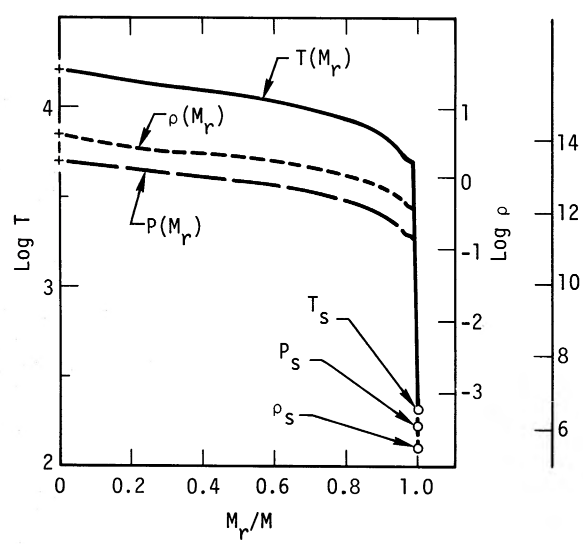

FIG. 6.—Radial variation of temperature, density, and pressure as a function of mass. These curves for S1 standard sequence epoch 4 are typical of the interior structure during the entire degenerate phase. The center (+) and surface (○) points are indicated.

relative contribution of gravitational and internal energy in supplying the luminous energy radiated. The early stellar phase is characterized by steadily increasing E_{grav} and E_{internal}, as shown in Figure 7 for the S1($T_0 = 102$ K) standard sequence. Both E_{grav} and E_{internal} increase monotonically until T_{max} is reached; with a small time lag (at $\log t \approx 5.18$) E_{internal} reaches a maximum, then starts to decrease. At the same epoch, the increase in E_{grav} changes to a less rapid rate, correlating with the previous demonstrated change in dR/dt (see Fig. 2). The gravitational energy source is dominant until epoch 2, then E_{internal} is called upon to supply an increasing proportion of the radiated energy. Over the period $6 \leq \log t \leq 8$,

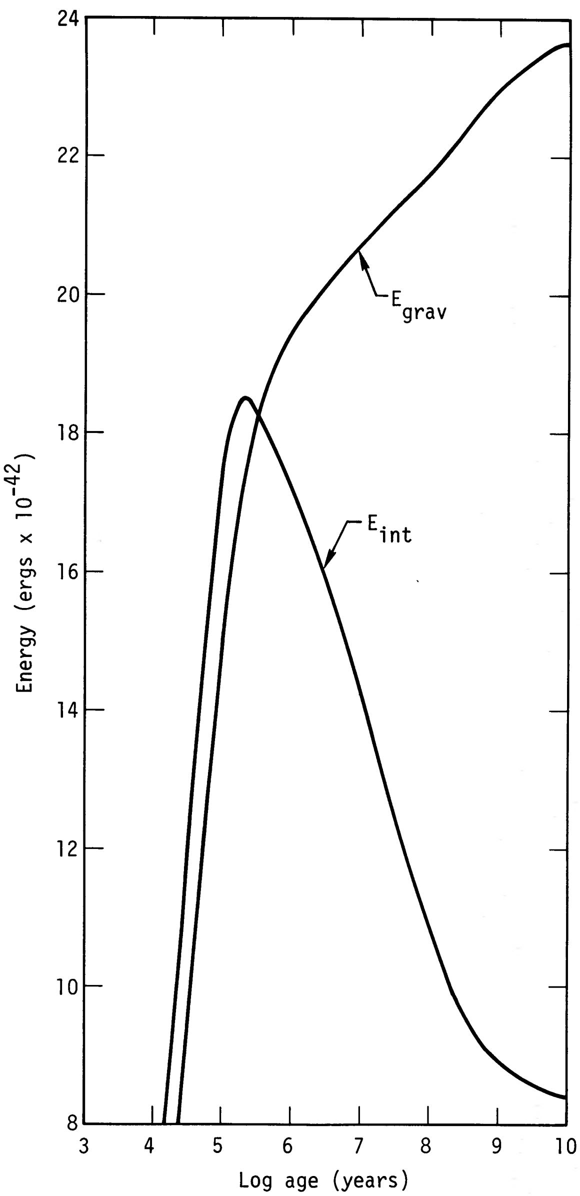

FIG. 7.—The gravitational and internal energy for the S1, $T_{\odot} = 102$ K model sequence.

E_{internal} supplies twice the energy that the gravitational source provides. As the planetary radius changes over to its late-time asymptotic behavior, E_{internal} also flattens out.

b) *Sensitivity Analysis*

A number of separate factors must be considered in assessing the validity of a stellar structure calculation. Five specific factors that affect the evolutionary sequence will be investigated in this section to determine the sensitivity of our results to changes or errors in any of these factors. The first and most obvious variable is the chemical composition, since it is the key parameter (together with the mass) that determines the entire evolutionary behavior of a star. A special feature, not encountered in usual stellar structure studies, is the exact value of the solar energy deposition, which requires a knowledge of the solar energy as a function of time as well as the time, angle, and wavelength variation of the planetary albedo. The third factor is the thermodynamic properties (equations of state and their derivatives), where errors or inadequate approximations can have a large influence on stellar structure. The fourth factor, the structure of the model atmospheres, enters into the surface boundary layer condition since the behavior of gravitationally contracting systems is completely controlled by the surface boundary layer. The fifth source of model variation is a different part of the surface condition, the structure and extent of the superadiabatic zone. These five elements are analyzed by calculating evolutionary model sequences that start from epoch 2 (T_{max}) values and continue to 10^{10} years. All test sequences were calculated with the S1 solar mixture composition (except for the pure hydrogen sequence) and with $T_{\odot} = 102$ K (except the study of $T_{\odot}$ variations).

The effect of varying the chemical composition is the most difficult to analyze because each composition requires construction of a complete set of thermodynamic properties and a complete set of model atmospheres. This was done for a system of pure hydrogen, and a sequence of pure H models calculated from 6.6 R_J to 10^{10} years. The results of this different composition are shown in Figures 1–4. The H sequence is essentially similar to the S1 sequence; it differs from the pure hydrogen model sequence described by Grossman *et al.* (1972) due to improvements in the hydrogen equations of state. As shown in Figure 1, the H sequence lies at lower L and lower T_e than the S1 sequence at the same epoch, the largest differences occurring during the period $4 \lesssim \log t \lesssim 7$. The observable variables R and L shown in Figures 2 and 3 are similar to the S1 case, with the H sequence radius being some 18 percent larger than R_J at 2.5×10^9 years but the luminosity being almost identical to the S1 value. The moderate differences in the observables also occur in the internal structure. In Figure 4 the H sequence exhibits low-mass-star and degenerate behavior, but is cooler and less dense than S1 at all times. The temperature maximum is only

30,600 K at $\log \rho = -0.03$, and this occurs at a later time, $\log t = 5.9$.

A more detailed picture of the effect of chemical composition differences is presented in Figures 8, 9, and 10. Figure 8 is an expanded diagram of the $(\log L, \log T_e)$-plane in the vicinity of L_J and $(T_e)_J$. The two observational points shown correspond to the values of L_J and $(T_e)_J$ for the values $T_\odot = 89$ K and 108 K. The rectangular boxes surrounding these points represent the observational error limits assigned by Aumann *et al.* (1969). The $(\log L, \log T_e)$-track for the S1 standard sequence ($T_\odot = 102$ K) is indistinguishable from the $T_\odot = 89$ K and 108 K tracks. The slight offset of the observational values from the S1 track is shown, being but a small fraction of the indicated observational error limits. The H sequence in Figure 8 lies at similar L but lower T_e than the S1 sequence at equal epochs, and is outside the error limits for both $T_\odot$ values. As seen here, the position of the (L, T_e)-track is relatively sensitive to composition, more so than any other physical parameter; this sensitivity will prove valuable in later studies in determining an accurate H/He ratio. The time dependence of radius illustrated in Figure 9 demonstrates that a pure or nearly pure hydrogen fluid model clearly cannot produce a model with the observed radius R_J. The first major study of Jupiter by DeMarcus demonstrated that a cold model composed

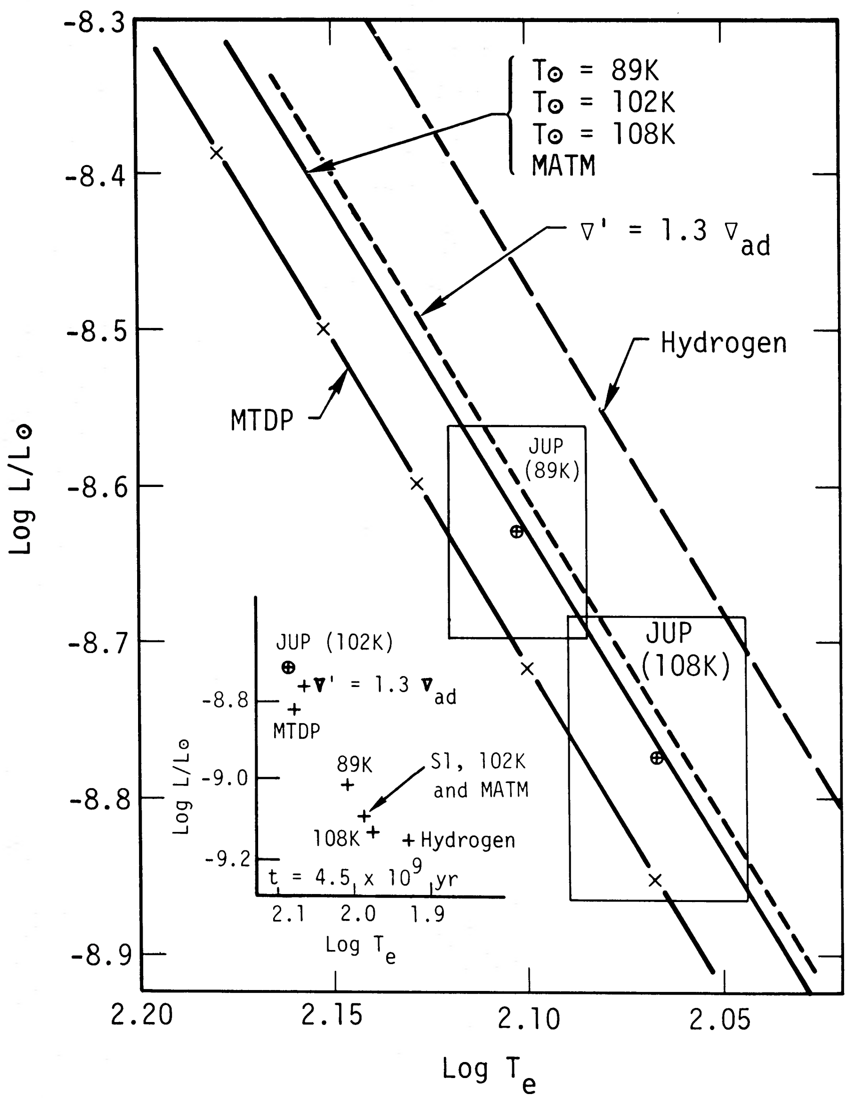

FIG. 8.—An expanded diagram of the $(\log L, \log T_e)$-plane in the vicinity of the observational values of L_J and $(T_e)_J$ for Jupiter. The observational values ($\oplus$) for Jupiter ($T_\odot = 89$ and 108 K) are shown along with the observational error limits given by the surrounding rectangular boxes. The solid curves (—) represent the S1 standard sequence with the insolation variations ($T_\odot = 89$ K, 102, 108 K) coinciding. The $(\log L, \log T_e)$-tracks are illustrated for the hydrogen sequence (— —), the modified thermodynamic properties sequence (—+—), and the superadiabatic sequences (---). The modified model atmospheres (MATM) sequence coincides with the S1 standard sequence. The inset shows the change from S1 standard sequence for each variation at $t = 4.5 \times 10^9$ years.

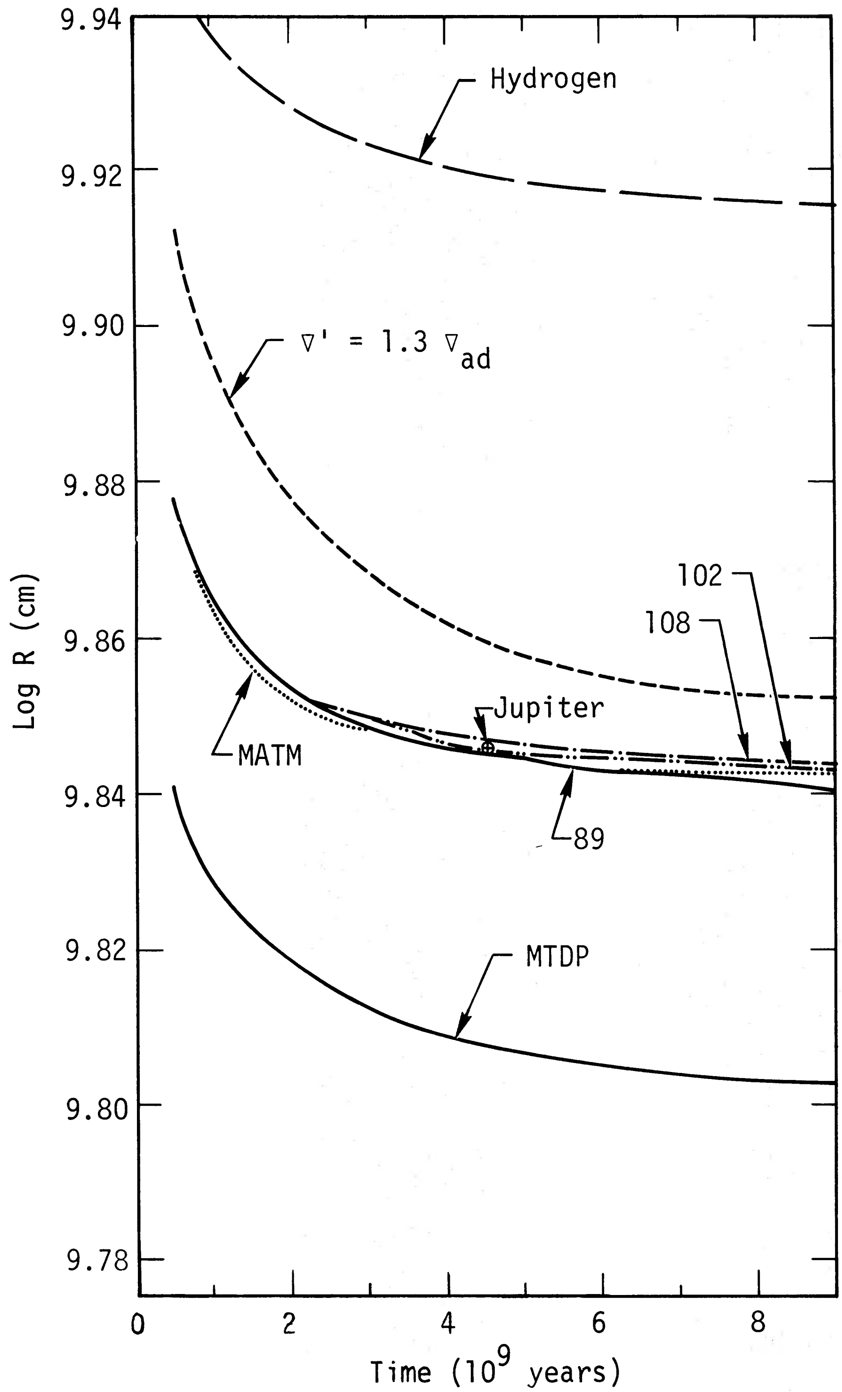

FIG. 9.—Variation of radius with time for various sequences. The S1 standard sequence ($T_\odot$ = 120 K) is shown together with $T_\odot$ variations, modified thermodynamics, modified atmospheres, hydrogen and superadiabatic zones. The value of R_J ($\oplus$) is shown at 4.5×10^9 years.

mainly of solid hydrogen must have a content of $X = 0.78$ to agree with the observations. From this study, a hot adiabatic fluid planet with $X = 0.74$ is found to give the best agreement with observations. The luminosity of the H sequence shown in Figure 10 is little different from the S1 sequence $L(t)$ curve; it is also lower by a factor of 2.85 than L_J at 4.5×10^9 years. Increasing the helium content of the models decreases R and increases T_e. The S1 solar mixture gives R_J and $(T_e)_J$ for a convective, fully mixed, adiabatic fluid model. Since other important factors as discussed below also have an influence on the

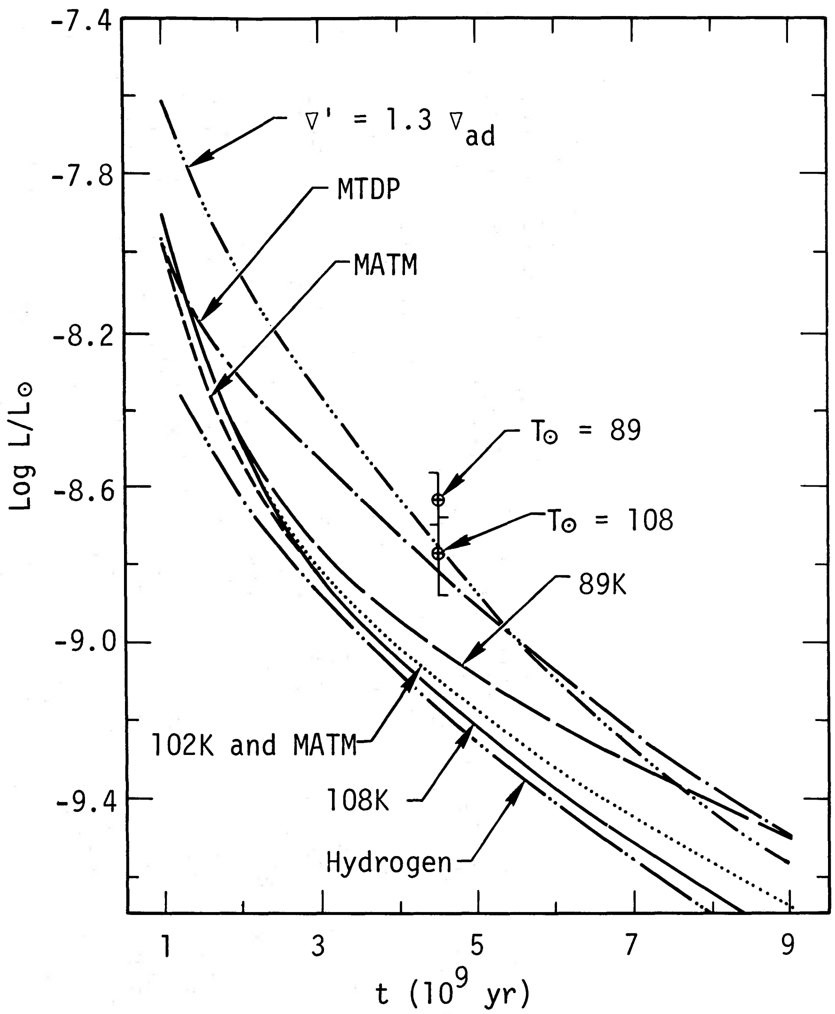

FIG. 10.—Variation of luminosity with time for various sequences. The 89 K, 108 K, and MATM sequences lie very close to the S1 standard sequence. The two values of L_J correspond to $T_\odot = 89$ K and 108 K.

models, we cannot state that Jupiter's composition is S1; it is probable that S1 is an upper limit ($X_J \leq 0.74$) and is close to the correct value.

The second parameter to be studied is the insolation temperature, that is, the effective solar energy deposition. The limiting values for Jupiter as discussed in § II are 89 and 108 K. In addition to these, an evolutionary sequence was calculated for $T_\odot = 3$ K, the temperature of the cosmic background, in order to represent a 0.00095 $M_\odot$ object evolving as a single star with no dominant companion such as the Sun. The effects of varying $T_\odot$ are interesting, as seen from Figure 8, 9, and 10. As shown in Figure 8, the change of $T_\odot$ has no effect on the location of the (log L, Log T_e)-track. The 3 K track (not shown) is closer to the 108 K track than to the observational values. The $T_\odot$ factor does have a large effect on the lifetimes of these models, however; smaller $T_\odot$ gives significantly longer contraction times. Variations in $T_\odot$ cause the (log L, log T_e)-track to be displaced parallel to its own direction, while the shift perpendicular to the track is very small. The effects on the observational variables R and L shown in Figures 9 and 10 are that for larger $T_\odot$ the models have a larger R and a smaller L at a given epoch. The changes only become substantial for times of the order of 10^9 years. Since T_e for log $t < 9$ is sufficiently larger than $T_\odot$, the solar contribution has no effect on the early evolution but begins to influence the sequence when the models have cooled so that $(T_\odot/T_e)^4$ is not negligible. The sensitivity of the radius to $T_\odot$ given in Figure 9 becomes very large for $t \gtrsim 2 \times 10^9$ years even though the absolute difference in radius is small. The sensitivity of model luminosity is more observable. The luminosity achieved at 4.5×10^9 years on the S1 standard sequence is reached in 4.3×10^9 years (108 K) and 5.13×10^9 years (89 K), giving an age variation of -4 percent to $+14$ percent. At $L = L_J$ on the S1 sequence, the corresponding times to this luminosity for the 108 K and 89 K sequence are 2 percent lower and 7.5 percent higher. Two conclusions are evident from this behavior: first, any reasonable value of $T_{\odot}$ used with the present model physics fails to give a lifetime approaching 4.5×10^9 years; second, in any study of Jupiter, or other contracting giant planet where $(T_{\odot}/T_e)^4$ is non-negligible, the exact value of $T_{\odot}$ is quite important in determining accurate time scale for late evolutionary stages. A final feature of the sensitivity of the model sequence to $T_{\odot}$ is illustrated in Figure 11 where the time dependence of T_c and ρ_c are plotted for the various $T_{\odot}$ sequences. The approach to $T_{\max}$, the subsequent cooling, and the steady increase in ρ_c, occur for all three values of $T_{\odot}$. Differences in internal structure only appear at $\log t \sim 9.3$, remaining small till $\log t \sim 10$. At all times ρ_c differs only by a percent, while only near the end of the track do the different $T_{\odot}$ tracks differ in T_c by as much as 17 percent. The shorter tracks for larger $T_{\odot}$ values are due to these model sequences evolving off the equation-of-state tables at earlier times.

The third sensitivity study involves the thermodynamic properties. As discussed in § II*b*, a set of S1 thermodynamic properties was constructed by introducing a perturbation function which added a predetermined factor to the nominally correct S1 results. This variation, the modified thermodynamic properties (MTDP), was used to calculate an evolutionary sequence from $T_{\max}$ to 10^{10} years, with $T_{\odot} = 102$ K. These results are also given in Figure 8, where they produce significant modifications in model behavior. The MTDP $(\log L, \log T_e)$-track is shifted toward larger L and larger T_e at the same epoch as S1, the shift being 21 percent in luminosity and 5 percent in T_e. The MTDP track lies farther away from the best observational values, yet is well within the observational error limits. Note that if this altered equation of state were accepted as the best model, a composition with less helium than S1 would be required to match the L_J, $(T_e)_J$ values. The major influence of the MTDP modification lies in its effect on the time scale of evolution. This can be seen from the time dependence of R and L, shown in Figures 9 and 10. The radius is smaller than R_J at 4.5×10^9 years by about 8 percent (it could be increased by a slight decrease in the He content); the luminosity, however, is much closer to the observational values, being only 27 percent below the observed current value. In terms of lifetime, a time of 3.95×10^9 years is required for the MTPD model to reach L_J. Another view of the relative effect of the MTDP is seen in the insert in Figure 8, where the change in predicted L, T_e at 4.5×10^9 years is illustrated. The large shift of MTDP relative to S1 is easily seen in this form; it not only shifts the position of the track, but has a much more pronounced shift along the track.

Clearly, the improved agreement with observation resulting from the MTDP calculation demonstrates the great sensitivity of the planetary evolution calculation to changes in the equation of state. This equation-of-state sensitivity also indicates that the thermodynamics of the interpolation region need to be reevaluated, with a stronger bias toward the metallic fluid result—or better yet, elimination of interpolated values and their replacement by an accurate treatment of the molecular metallic interface.

A similar estimate of errors and uncertainties was carried out for the model atmospheres used in this study, as discussed in § II. The resulting modified model atmospheres (MATM) were used to calculate an evolutionary sequence as for the MTDP case. The results of the MATM sequence differ negligibly from the S1 standard sequence; the sensitivity of the S1 sequence to errors or changes in the model atmospheres are by far the smallest of the five factors studied here. The MATM $(\log L, \log T_e)$-track in

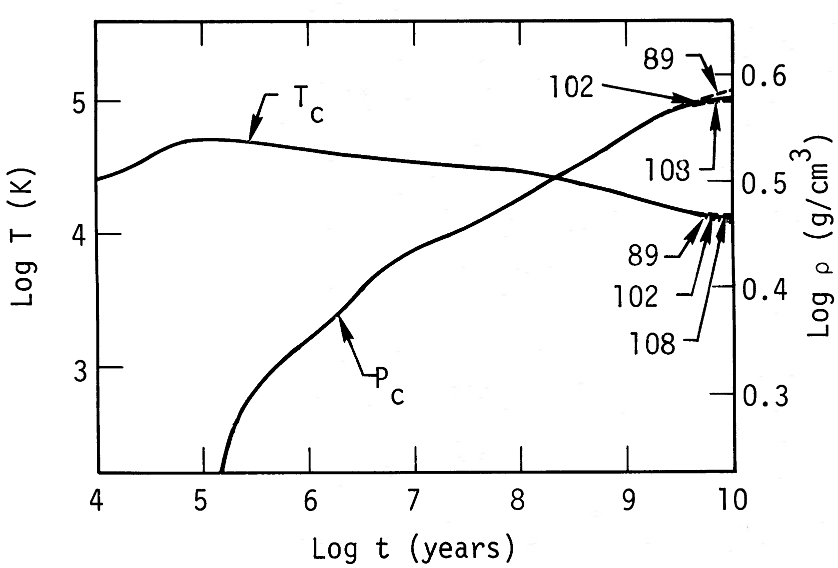

FIG. 11.—Variation of S1 sequence central temperature and density with time. The effects produced by varying $T_{\odot}$ are noticeable only for $\log t \gtrsim 9.3$.

Figure 8 coincides with the standard sequence, while the slight difference in the time dependence of the radius is shown in Figure 9. The luminosity (Fig. 10) drops 15 percent below S1 at most; usually the difference is 1 percent or less. Unless errors which are far larger than we have estimated are present, the current set of model atmospheres is sufficient for accurate analysis of the Jovian system.

The final sensitivity study concerns the incorporation of a superadiabatic zone in the surface boundary layer of the models. All prior studies of Jupiter (including this study up to this point) have proceeded on the assumption that completely adiabatic models are sufficient to treat the problem of giant planet structure. A recent paper (Hubbard 1973) suggests that an accurate representation of the internal temperature distribution of Jupiter can be obtained by a careful determination of the entropy of the outer layers of the planet. The accuracy of prior Jovian models and the feasibility of Hubbard's experiment depend alike on the assumption of complete adiabaticity of the giant planets. This assumption is open to serious question. It is well known that main-sequence stars contain superadiabatic regions in their outer envelopes, and for the fully convective stars of the lower main sequence which constitute the closest stellar configuration to these planetary models, this superadiabatic zone is the key structural feature in determining the luminosity or energy release rate of the object. For example, a recent study of the lowest mass thermonuclear stars (Grossman and Graboske 1973), including masses as small as $0.008\ M_\odot$ ($\sim 9\ M_J$), significant superadiabatic zones were found throughout the entire gravitational contraction phase.

Since a superadiabatic zone could conceivably exist for the $0.00095\ M_\odot$ model, we have attempted to assess its importance. An exact calculation using mixing-length theory with the necessary theoretical physical details is a major undertaking, so a rough approximation was used to determine if the evolutionary sequence is indeed sensitive to this feature. From the mixing-length theory of convective transport with specific structural details taken from the closest stellar analogs (the low-mass deuterium main-sequence models, $M \sim 0.01\ M_\odot$) a pseudo-superadiabatic zone was created. This zone was restricted to the range $-5.5 \leq \log \rho \leq -3$, a density range which incorporates only 10^{-4} of the total stellar mass for the Jovian model. In this zone, the effective superadiabatic temperature gradient ∇' was approximated by equating it to $n \cdot \nabla_{\rm ad}$, where n was estimated from the low-mass star analogs to be 1.3. An evolutionary sequence was calculated for this superadiabatic case, and the results are shown in Figure 8. The ($\log L$, $\log T_e$)-track is shifted significantly for $\nabla' = 1.3\nabla_{\rm ad}$ toward higher L and higher R at the same epoch relative to the S1 standard sequence. The $\nabla' = 1.3\nabla_{\rm ad}$ sequence lies close to the S1 sequence, in the H-R diagram lying well within the observational error limits. The sensitivity of the sequence to superadiabatic effects is shown more clearly in the inset to Figure 8, Figures 9 and 10. In Figure 9, the $\nabla' = 1.3\nabla_{\rm ad}$ sequence approaches R_J at 4.5×10^9 years (3 percent too high) and appears to approach R_J as a limit. These substantial effects on the radius are surpassed by the sensitivity of the luminosity to ∇', illustrated in Figure 10. The $\nabla' = 1.3\nabla_{\rm ad}$ has $L = 0.88 L_J$ at 4.5×10^9 years, much closer than the S1 sequence. Another interpretation is that $L = L_J$ at $t = 4.35 \times 10^9$ years, a 65 percent increase in the lifetime. The interior structure of the superadiabatic sequence is equally sensitive to ∇'. The $\nabla' = 1.3\nabla_{\rm ad}$ sequence has a central temperature at 4.5×10^9 years of 18,900 K, about 27 percent higher than the S1 standard model at the same epoch. This increased internal temperature would decrease the onset of gravitational separation and reduce the possibility of solidification, so that onset of solid phases in these models would be delayed, for example, to $t > 10^{10}$ years for the case studied here. In conclusion, the extreme sensitivity of the fluid models to the presence of a superadiabatic zone is a significant effect; its real contribution should be determined by a careful quantitative study, if only to eliminate it from further consideration.

In summary, the evolutionary calculations for models composed of fully mixed, convective, adiabatic fluid undergoing quasi-static gravitational contraction yield a standard sequence in agreement with the observed luminosity and radius of Jupiter. Reasonable variations in chemical composition, thermodynamic properties, atmosphere structure, and solar energy deposition produce different perturbations of the standard sequence, all lying within the observational error limits. The major problem is that the adiabatic homogeneous fluid models have a short time scale for contraction to L_J, approximately 3 to 4×10^9 years. The great sensitivity of the fluid models to the equation of state and to the presence of a superadiabatic zone could alter this situation, and clarification of these factors must be included before a final evaluation of the fluid contraction stage is possible.

The energy source for the luminosity for all models subsequent to the occurrence of the central temperature maximum is a combination of gravitational energy and internal energy. The steady cooling of the interior demonstrates that a substantial fraction of the luminosity arises from the internal heat stored during the early stellar phase, prior to the temperature maximum. From the behavior of the radius-time curves (Fig. 9, also Fig. 7) the gravitational energy contribution for the standard model becomes relatively small for the period 10^6–10^9 years. A definitive measure of the internal and gravitational energy contributions must await the improved thermodynamics and complete superadiabatic treatment of the fluid model.

At this point, a brief assessment of the consistency and validity of the basic assumptions can be made. The internal temperatures existing throughout the standard evolutionary sequence clearly support the concept of a hot convective fluid which remains fully mixed from center to surface at all times. Kieffer (1967) has investigated the differences between spherical and rotating (nonspherical) planetary models, and finds that the effect of including rotation in models of present-day Jupiter is a 1.38 percent increase in radius. This indicates that the assumptions of negligible rotation and spherical symmetry will not alter the observational predictions by more than 1 or 2 percent.

IV. DISCUSSIONS AND CONCLUSIONS

The most interesting result of the early evolution is the existence of a high-luminosity phase ($-2 \leq \log L/L_\odot \leq -4$) during the fluid contraction. This high luminosity would have a very strong influence on the formation of the Jovian satellites, as well as perhaps on the formation of outer solar system planets. The expected consequence of a high-luminosity phase would be depletion of the volatile (low Z) materials in the surrounding nebula, just as is postulated for the inner solar nebula. This depletion would be apparent in the structure of the Jovian satellites, in the form of higher mean densities for the inner satellites formed from the most depleted material. In fact, just such a decreasing mean density dependence is observed in Galilean satellites, from 2.8 g cm^{-3} to 1.5 g cm^{-3} (Cameron 1973). This radial mean density gradient in the Jovian satellites is a very convincing observational indicator of the occurrence of a high-luminosity phase of the central object. This subject will be examined in detail elsewhere (Pollack and Reynolds 1974). An additional consideration for early solar system evolution is that the occurrence of this phase for both Jupiter and Saturn at early times would produce two radiation sources in the outer solar nebula with luminosities equivalent to late M dwarf stars.

A second interesting aspect of the early evolution is the high internal temperatures which exist throughout the model interiors for substantial periods corresponding partially to the high-luminosity stellar phase. As noted earlier, high internal temperatures ($T_c \geq 20{,}000$ K) exist even for a fluid system as small as 1.14 R_J. In such an environment, fluidization and mixing of inhomogeneous solids accreted during the planetary assembly phase would be complete. The relatively high temperature, convective, metallic fluid interior present for times approaching 10^{10} years is consistent with a second observational feature of Jupiter, the strong magnetic field. The results obtained here support Hubbard's (1968) conclusions concerning the temperature-driven dynamo model for field generation.

The extent of the high internal temperature phase (as well as the associated but shorter high-luminosity phase) depends on the mode of formation of the protoplanet. A typical protostar formation, from a collapsing diffuse cloud of gas and dust, would produce exactly the results described in § III. Objections to such a protostar collapse origin for Jupiter (Hills 1971) arise from considerations of tidal instabilities in the condensing protoplanetary nebula, induced by the solar gravitational field. Alternative formation mechanisms proposed are cold accretion (Hills 1971) and cold condensation (Horedt 1972). A possible problem with the instability arguments is that assumptions must be made about the mean density and temperature of the outer solar nebula. The timing of the high-luminosity phase of solar formation which could produce much higher temperatures throughout the solar system, as well as the possible presence of a hot protoplanet (unless Jupiter and Saturn are coeval, one of these objects passed through a high-luminosity phase while the other was still forming) both would produce (ρ, T)-conditions significantly different from those postulated assuming that a main-sequence Sun existed at the time of planetary formation. Another feature of the Jupiter and Saturn systems which would be a natural consequence of a protostar origin, but not necessarily of a cold origin, is the presence of a large number of satellites. Just as the planets formed from the nebular disk left by the contracting proto-Sun, so the planetary nebulae of Jupiter and Saturn would produce a number of compact remnants. We feel that a protostar collapse origin, while subject to serious difficulties as discussed by Hills, is not ruled out given the uncertainties concerning the actual densities and temperatures present in the early solar nebula. A recent study which supports this conclusion (Bodenheimer 1974) performs a hydrodynamic calculation for the early evolution of Jupiter. This dynamic model sequence includes details of a realistic protostar collapse, terminating in a quasi-static model with a radius of 4–5 R_J and a temperature of approximately 30,000 K. The agreement with the model sequence in this study, near epoch 2, is reasonable, given the differences in composition and physics.

However, if a cold origin—accretion or condensation—is accepted for Jupiter, does this rule out the existence of a high-luminosity phase? As the core object accumulates mass so that $M \to M_J$, the large amount of gravitational energy released would, following the virial theorem, be converted into internal heat. This heat would soon increase internal temperatures beyond the 1000–1500 K range currently estimated to cover the melting temperature of metallic solid hydrogen. Once the hydrogen lattice begins to melt, the protoplanet would rapidly relax into a fully fluid structure, and from its point of initial relaxation onto the fluid quasi-static contraction track it would again follow exactly the evolution of § III. While it seems evident that an accretion-condensation object will relax to a fluid system as $M \to M_J$, the actual details of this process will be complex, and will require a more difficult evolutionary calculation than the fluid contraction models studied in this paper. A subsequent paper will report on a detailed study of the accretion-condensation-relaxation process in an attempt to understand better the formation of the giant planets.

The third stage of Jovian evolution, post–fluid contraction, is equally complex and equally unknown at present. Its actual relevance to the study of Jupiter and Saturn cannot be determined until an accurate model of the fluid contraction stage is completed. This final determination requires an unambiguous model calculation with minimal uncertainty in the fluid constitutive physics. The results of § III yield an S1 evolutionary time for fluid contraction to R_J, L_J of $t = 2.6 \times 10^9$ years, with a range of 2.6 to 4.35×10^9 years' variation produced by changes in chemical composition, model atmospheres, superadiabaticity, thermodynamics, and solar energy deposition. Since the time scale for either theory of the formation stage, accretion (10^6 years) or collapse (10^2 years), has a negligible influence on the time scale, there are various explanations for this short fluid time scale. Either Jupiter is less than 4.5×10^9 years old (very unlikely), the fluid contraction stage is superadiabatic (possible), the thermodynamic properties are sufficiently different from those of the S1 model (very probable), or there is a substantial post–fluid contraction stage (possible).

At least three physical mechanisms have been proposed which would explain a post-fluid contraction phase. Smoluchowski (1967) has pointed out that solidification of hydrogen, with consequent release of the latent heat of crystallization, would provide a major energy source. In addition, he suggests that following solidification of the hydrogen, the interstitial neutral helium fluid would be gravitationally differentiated, producing a primarily fluid helium region adjacent to a primarily solid hydrogen region, with the gravitational energy from the segregated materials providing an additional energy source. A related hypothesis, recently proposed by Salpeter (1973), proposes that the neutral helium fluid becomes immiscible with the metallic hydrogen fluid. The subsequent gravitational differentiation again unmixes the two materials and releases a large amount of gravitational energy. All these late-stage hypotheses would provide sufficient energy release to explain L_J with greatly reduced or even zero contraction required, hence the description "post–fluid contraction."

Although the third stage must eventually occur at some late epoch (solidification of the mixture will occur as T approaches the freezing temperature), it is not necessarily required to explain the structure of the current epoch planet. To demonstrate the presence of a post–fully mixed fluid structure requires, first, that a realistic physical theory of the material behavior be developed, and second, that the planetary fluid contraction phase proceeds to the point in time and (ρ, T)-space where these solidification or separation processes occur. Thus the presence of this post–fluid contraction stage will depend crucially on the exact structure and time scale of the fluid contraction stage. For example, if the fluid phase lasts for 5×10^9 years before solidification or separation ensues, the immediate need to physically model this process is reduced. The internal structure and time scale of the fluid contraction phase were shown, in § III*b*, to be sensitively dependent on the equation of state and on the existence and structure of a planetary superadiabatic zone. According to the sensitivity analysis, inclusion of improved thermodynamics (in better agreement with Monte Carlo results) will increase the time scale at all epochs of the fluid sequence, and will increase the temperature throughout the interior. Both these effects will delay the onset of a post–fluid contraction stage, possibly for very long times.

A consideration of the time required to reach a given luminosity can lead to a demonstration that improved thermodynamics and superadiabaticity are each capable of extending the age of the fluid contraction phase. From the derivation given in the Appendix, the time to reach a specified luminosity L for a spherical system of mass M and radius R is

$$t_L = \left(\frac{P_i}{P_a}\right)^{\eta} \frac{\langle C_V \rangle M}{4\pi R^2 \sigma} \int_{T_a(1)}^{T_a(2)} \frac{dT_a}{T_a^{\,4} - T_\odot^{\,4}}\,,$$

where t_L is dependent on the mean specific heat $\langle C_V \rangle$, the ratio of mean interior pressure P_i to the pressure at optical depth unity P_a, raised to the power η, a mean value of the gradient. The only quantities affecting t_L are P_i/P_a, η, and $\langle C_V \rangle$; and the value for t_{L_J} obtained for the standard sequence is 0.58 times the observed value. The ratio P_i/P_a changes very little between epochs 3 and 5 ($\log t = 6.18$ to 10), as can be seen from the (ρ, T)-structure lines in Figure 5. Both $\langle C_V \rangle$ and (P_i/P_a) can be strongly influenced by changes in the equation of state, so changes such as MTDP can have a strong effect on t_L. Clearly, if the interior has substantial subadiabatic (radiative or conductive) regions, the value of η would be lower and the fluid contraction would be even shorter. The values of $\langle C_V \rangle$ and (P_i/P_a) are mass averages, but η is weighted more toward the outer envelope where most of the change in temperature occurs. To increase t_L by 2 or more, η must be increased by about 50 percent in the outer envelope. This effect would be produced by the introduction of an outer-envelope superadiabatic zone. In conclusion, the most important task in the continuing evolutionary study of giant planets is a careful revision of the equation of state and an investigation of the existence of a superadiabatic zone. Once these modifications have been included in an evolutionary calculation, it will be possible to assess the need for, and the occurrence of, post–fluid contraction stages of planetary evolution.

One of the authors (A. S. G.) would like to acknowledge support for this work from NSF grant GP-25949. This work was supported in part by the Office of Planetology Programs, NASA.

APPENDIX

The degenerate phase composes the majority of the planetary lifetime, and the internal energy is an important energy source throughout this phase. Let us equate the luminosity due to the self-energy to the rate of change of internal energy,

$$L = -dU/dt \tag{A1}$$

where L is related to the total effective temperature T_e and the solar component $T_\odot$ by

$$L = 4\pi R^2\sigma(T_e^4 - T_\odot^4)\,, \tag{A2}$$

where σ is the Stefan-Boltzmann constant and R the planetary radius. For late epochs, R and $T_\odot$ are considered time-independent, and T_e is set equal to the atmospheric temperature near optical depth unity. Furthermore, the internal energy is written as

$$U = \langle C_V \rangle T_i M \tag{A3}$$

where $\langle C_V \rangle$ is a mean specific heat for the planetary interior, T_i is a mean interior temperature, and M is the total mass.

Combining (1), (2), and (3), the time to cool from state 1 to state 2 is

$$t_L = \frac{\langle C_V \rangle M}{4\pi R^2\sigma}\int_1^2 \frac{dT_i}{(T_i^4 - T_\odot^4)}\,, \tag{A4}$$

where we have neglected the variation of $\langle C_V \rangle$ with time. The quantities T_a and T_i are related by a mean gradient η,

$$T_i = (P_i/P_a)^\eta T_a\,, \tag{A5}$$

where P_i and P_a are the pressures at temperatures T_i and T_a. Combining equations (A4) and (A5), we find that t_L is given approximately by

$$t_L = \left(\frac{P_i}{P_a}\right)^\eta \frac{\langle C_V \rangle M}{4\pi R^2\sigma}\int_{T_a(1)}^{T_a(2)} \frac{dT_a}{(T_a^4 - T_\odot^4)}\,. \tag{A6}$$

For $T_a(1)$ much larger than $T_a(2)$, as is the case for the degenerate phase, the integral will be a function of $T_a(2)$ only. Thus the time to reach a specific luminosity is only a function of the quantities appearing outside the integral in Equation (A6).

REFERENCES

Allen, C. W. 1963, *Astrophysical Quantities* (London: Athlone).
Aumann, H. H., Gillespie, C. M. Jr., and Low, F. J. 1969, *Ap. J.* (*Letters*), **157**, L69.
Bodenheimer, P. 1974, *Icarus*, **23**, 319.
Burch, D. E., Gryvnak, D. A., France, W. L., and Williams, D. 1962, *Report 62-698* (Air Force Cambridge).
Cameron, A. G. W. 1973, *Science*, **180**, 701.
DeMarcus, W. 1958, *Ap. J.*, **63**, 2.
Ezer, D., and Cameron, A. G. W. 1963, *Icarus*, **1**, 422.
Ferriso, C. C., Ludwig, C. B., and Thomson, A. L. 1966, *J. Quant. Spectrosc. and Rad. Transfer.*, **6**, 241.
France, W. L., and Williams, D. 1964, *Report 64-652* (Air Force Cambridge).
Gille, J. C., and Lee, T. H. 1969, *J. Atm. Sci.*, **26**, 932.
Graboske, H. C. Jr., Olness, R. J., and Grossman, A. S. 1975, *Ap. J.*, **199**, 255.
Grossman, A. S., and Graboske, H. C. Jr. 1973, *Ap. J.*, **180**, 195.
Grossman, A. S., Graboske, H. C. Jr., Pollack, J. B., Reynolds, R., and Summers, A. 1972, *Phys. Earth Planet. Interiors*, **6**, 91.
Hills, J. G. 1971, *Bull. AAS*, **3**, 481.
Horedt, G. P. 1972, *Ap. and Space Sci.*, **15**, 129.
Hubbard, W. B. 1968, *Ap. J.*, **152**, 745.
———. 1969, *ibid.*, **155**, 333.
Hubbard, W. B. 1970, *Ap. J.*, **162**, 687.
———. 1972, *ibid.*, **176**, 525.
———. 1973, *Ap. J.* (*Letters*), **182**, L35.
Hubbard, W. B., and Slattery, W. L. 1971, *Ap. J.*, **168**, 131.
Hubbard, W. B., and Smoluchowski, R. 1973, *Space Sci. Rev.*, **14**, 599.
Irvine, W., Simon, T., Menzel, D. H., Pikoos, C., and Young, A. T. 1968, *Ap. J.*, **73**, 807.
Kieffer, H. H. 1967, *J. Geophys. Res.*, **72**, 3179.
Kippenhahn, R., Weigert, A., and Hofmeister, E. 1967, *Methods in Computational Physics*, Vol. 7, *Astrophysics*, ed. B. Alder (New York: Academic Press).
Linsky, J. L. 1969, *Ap. J.*, **156**, 989.
Newburn, R. L., Jr., and Gulkis, S. 1973, *Space Sci. Rev.* **3**, 179.
Peebles, P. J. E. 1964, *Ap. J.*, **140**, 328.
Pollack, J. B. 1969, *Icarus*, **10**, 301.
Pollack, J. B., and Ohring, G. 1973, *Icarus*, **19**, 34.
Pollack, J. B., and Reynolds, R. T. 1974, *Icarus*, **21**, 248.
Salpeter, E. E. 1973, *Ap. J.* (*Letters*), **181**, L83.
Smoluchowski, R. 1967, *Nature*, **215**, 691.
———. 1970, *Science*, **168**, 1340.
———. 1972, *Physics of the Solar System* (NASA SP-300), p. 271.
Trafton, L. 1967, *Ap. J.*, **147**, 765.

H. C. Graboske and R. J. Olness: Lawrence Livermore Laboratory, L-504, P.O. Box 808, Livermore, CA 94550

A. S. Grossman: Department of Physics, Iowa State University, Ames, IA 50010

J. B. Pollack: Space Sciences Dvision MP-245-3, NASA/Ames Research Center, Moffett Field, CA 94035